Biophys Rep 2019, 5(5–6):254–263
https://doi.org/10.1007/s41048-019-00100-y

Biophysics Reports

RESEARCH ARTICLE

Regulation of intracellular Ca^{2+}/CaMKII signaling by TRPV4 membrane translocation during osteoblastic differentiation

Fen Hu[1], Yali Zhao[1], Zhenhai Hui[1], Fulin Xing[1], Jianyu Yang[1], Imshik Lee[1], Xinzheng Zhang[1,2], Leiting Pan[1]✉, Jingjun Xu[1,2]

[1] The Key Laboratory of Weak-Light Nonlinear Photonics, Ministry of Education, School of Physics and TEDA Institute of Applied Physics, Nankai University, Tianjin 300071, China
[2] Collaborative Innovation Center of Extreme Optics, Shanxi University, Taiyuan 030006, Shanxi, China

Received: 10 June 2019 / Accepted: 11 August 2019 / Published online: 22 November 2019

Abstract Bone constantly remodels between resorption by osteoclasts and formation by osteoblasts; therefore the functions of osteoblasts are pivotal for maintaining homeostasis of bone mass. Transient receptor potential vanilloid 4 (TRPV4), a type of mechanosensitive channel, has been reported to be a key regulator in bone remodeling. However, the relationship between TRPV4 and osteoblast function remains largely elusive. Only little is known about the spatial distribution change of TRPV4 during osteoblastic differentiation and related signal events. Based on three-dimensional super-resolution microscopy, our results clearly showed a different distribution of TRPV4 in undifferentiated and differentiated osteoblasts, which reflected the plasma membrane translocation of TRPV4 along with prolonged differentiation. GSK1016790A (GSK101), the most potent agonist of TRPV4, triggered rapid calcium entry and calmodulin-dependent protein kinase II (CaMKII) phosphorylation via TRPV4 activation in a differentiation-dependent manner, indicating that the abundance of TRPV4 at the cell surface resulting from differentiation may be related to the modulation of Ca^{2+} response and CaMKII activity. These data provide compelling evidences for the plasma membrane translocation of TRPV4 during osteoblastic differentiation as well as demonstrate the regulation of downstream Ca^{2+}/CaMKII signaling.

Keywords Osteoblasts, Differentiation, TRPV4 channel, Plasma membrane translocation, Super-resolution microscopy, Ca^{2+} signaling

INTRODUCTION

Bone is a dynamic tissue that undergoes continuous remodeling between formation of new bone matrix by osteoblasts and resorption of preexisting bone matrix by osteoclasts (Crockett *et al.* 2011). A proper balance between osteoblasts and osteoclasts is vital for maintaining bone construction and function (Raggatt and Partridge 2010). Attenuation of osteoblast formation may lead to bone loss, osteoporosis, and eventually debilitating fractures (Zaidi 2007). Osteoblasts originate from mesenchymal progenitors that, with the appropriate stimulation, differentiate into preosteoblasts and then to mature, functional osteoblasts (Kassem *et al.* 2008). Mature osteoblasts express many biochemical markers and transcription factors (Gundberg 2000; Marie 2008). By undergoing extracellular matrix maturation and mineralization, osteoblasts form bone-like mineralized nodules *in vivo* and *in vitro* (Blair *et al.* 2017). An increase in proliferation results in a greater number of bone-forming cells, whereas increased differentiation enhances the capability

Electronic supplementary material The online version of this article (https://doi.org/10.1007/s41048-019-00100-y) contains supplementary material, which is available to authorized users.

✉ Correspondence: plt@nankai.edu.cn (L. Pan),

of osteoblasts to synthesize and secrete osteoid matrix. Therefore, osteoblastic differentiation plays essential roles in bone formation and mineralization, which can be regulated by various signals including hormones, cytokines, and external factors such as mechanical loading (Katagiri and Takahashi 2002; Long 2011).

Mechanotransduction has been recognized as one of the major factors regulating bone remodeling (Ehrlich and Lanyon 2002); however, it is still unclear how bone cells perceive this type of stimulation. It has been established that mechanical stimulus activates some mechanosensitive cation channels particularly the transient receptor potential (TRP) channels on the plasma membrane (Christensen and Corey 2007; Maycas *et al.* 2017). In the TRP superfamily, Transient receptor potential vanilloid 4 (TRPV4) is predominantly expressed in various types of bone cells including osteoblasts and serves as a potential "mechanosensor" (Abed *et al.* 2009; Guilak *et al.* 2010). As a type of polymodal channel, TRPV4 is capable of sensing multiple stimuli from the environment, such as heat, hypotonicity, acidity, and endogenous lipids downstream of arachidonic acid metabolism besides mechanical force (Garcia-Elias *et al.* 2014; White *et al.* 2016). Opening of TRPV4 channels will lead to increase in the intracellular Ca^{2+} concentration owing to Ca^{2+} influx, thereby acting as a central player in calcium signaling (Nilius *et al.* 2004). The role of TRPV4 in bone cells has been studied primarily using osteoclasts and chondrocytes (Masuyama *et al.* 2008; O'Conor *et al.* 2014). For instance, TRPV4-mediated calcium influx was found to regulate the terminal differentiation of osteoclasts (Masuyama *et al.* 2008), and the activation of TRPV4 was responsible for promoting chondrogenesis through a Ca^{2+}/calmodulin pathway (O'Conor *et al.* 2014). Furthermore, accumulating evidences indicated that TRPV4 mutations were linked to a variety of skeletal dysplasias (Kang *et al.* 2012; Leddy *et al.* 2014). These studies potently supported the fundamental importance of TRPV4 in normal bone remodeling. However, previous work showed conflicting data regarding the participation of TRPV4 in osteoblast functions. Some studies proposed that TRPV4 repressed alternative mesenchymal differentiation pathways such as adipocyte and chondrocyte differentiation, while it promoted osteoblast proliferation, differentiation and mineralization activity, and blocked osteoblast apoptosis (Kang *et al.* 2012; O'Conor *et al.* 2013). In contrast, there are reports suggesting no influence (Masuyama *et al.* 2008) or even an inhibitory effect (van der Eerden *et al.* 2013) of TRPV4 on osteoblast functions. Notably, a recent work revealed that osteoblastic differentiation enhanced the expression level of TRPV4, which is required for calcium oscillation induced by fluid flow (Suzuki *et al.* 2013).

Therefore, in the present study, we aimed to determine the distribution change of TRPV4 channels during osteoblast differentiation and then investigated how it influenced the cellular responses and signal transduction. Based on three-dimensional (3D) super-resolution microscopy, our results directly and visually revealed the plasma membrane translocation of TRPV4 in differentiated osteoblasts. Moreover, we found that the recruitment of TRPV4 to the membrane resulted from differentiation regulated downstream Ca^{2+}/calmodulin-dependent protein kinase II (CaMKII) signaling.

RESULTS

Osteoblastic differentiation enhanced the membrane protein expression of TRPV4

Firstly, we detected the expressions of TRPV4 in the isolated rat calvarial osteoblasts at different stages of differentiation (cells grown to differentiate in osteogenic medium for 0, 1, 3, 5, 7 days). As shown in Fig. 1A, the mRNA expression of TRPV4 was relatively low in undifferentiated osteoblasts (day 0). In contrast, the levels of TRPV4 mRNA were increased in parallel to the increase in differentiation, which corroborated previous findings (Suzuki *et al.* 2013), which somehow declined on day 7. Meanwhile, the mRNA levels of pacsin3, a protein that has been reported to modulate the membrane localization of the TRPV4 (Cuajungco *et al.* 2006), were also potently elevated during differentiation (Fig. 1B). We further examined the membrane and cytoplasmic protein expression of TRPV4 by Western blotting. Results showed that the membrane protein level of TRPV4 in osteoblasts was robustly enhanced along with prolonged differentiation, achieving maximum on day 3 and remaining constant thereafter on day 5 and day 7 (Fig. 1C and D). Accordingly, TRPV4 protein expression in the cytoplasm was gradually reduced upon differentiation (Fig. 1C and D). It exhibited a double band of TRPV4, which was considered to be the glycosylated form of TRPV4 from previous work (Xu *et al.* 2006). Besides, the osteoblastic differentiation on day 5 has been demonstrated by testing the expression level of marker genes of osteoblast differentiation (supplementary Fig. S1).

3D-STORM imaging demonstrated the plasma membrane translocation of TRPV4 channels during osteoblastic differentiation

Based on 3D-STORM, we clearly visualized the nanoscale spatial distribution of TRPV4 channels in osteoblasts.

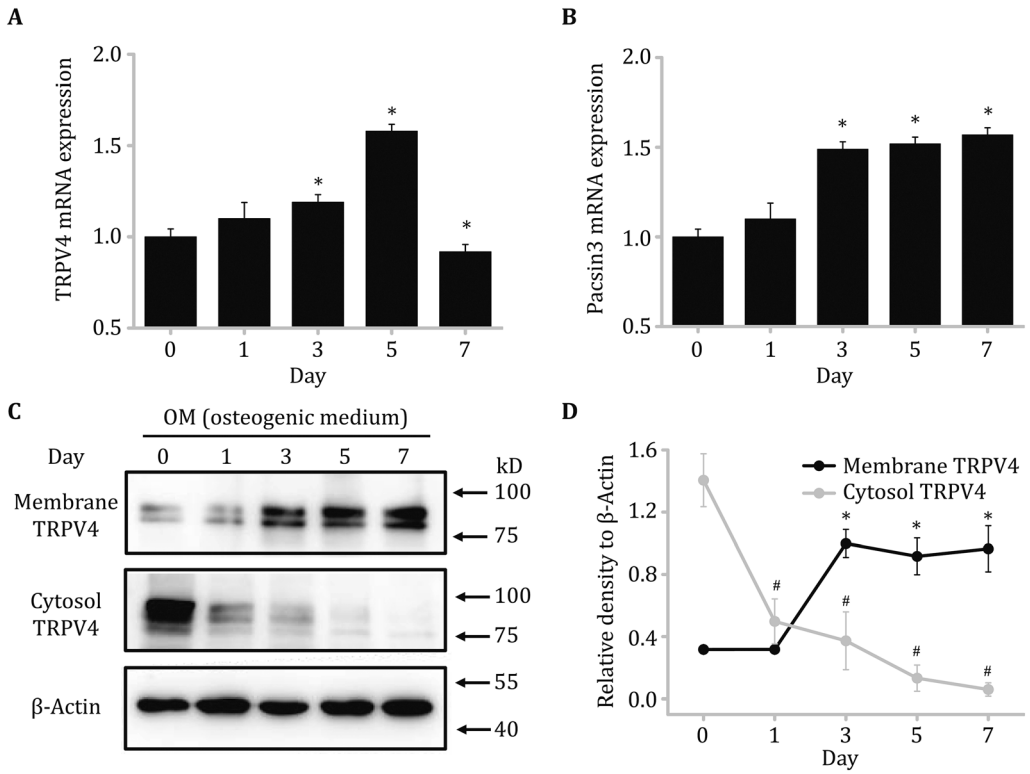

Fig. 1 The expression and distribution of TRPV4 in rat calvarial osteoblasts during differentiation. **A** TRPV4 mRNA expression analyzed by qRT-PCR in osteoblasts at different stages of differentiation (n = 3 for each case). Fold gene expression was determined by first normalization to GAPDH and then normalization to day 0 group. * indicates $P < 0.05$ comparing with day 0 group. **B** Pacsin3 mRNA expression analyzed by qRT-PCR in osteoblasts at different stages of differentiation (n = 3), * indicates $P < 0.05$ comparing with day 0 group. **C** Western blotting assay indicated an upward trend in expression of membrane TRPV4 protein and a downward trend in cytoplasmic TRPV4 protein along with osteoblast differentiation. **D** Quantitative statistical results of Western blotting normalized to the density of β-Actin (n = 3), * and # indicate $P < 0.05$ comparing with day 0 group

Representative STORM images from undifferentiated and differentiated groups are shown in Fig. 2 and supplementary Fig. S2, which potently improved the lateral and axial resolution compared with conventional images. In the undifferentiated group (day 0), we only observed a single-layer distribution of TRPV4 from the z direction (Fig. 2Ad). Gaussian fit of the count data acquired by STORM imaging also depicted a single-peak profile that quantitatively confirmed this single-layer distribution (Fig. 2Ae and Af). However, TRPV4 in differentiated cells (day 5) showed a distinct arrangement of two vertically separated layers, which was also verified by the two-peak Gaussian fit curves (Fig. 2B). The two layers can be spaced apart by more than 400 nm (Fig. 2Be and Bf). Correspondingly the structure of the cell body from z direction, and the upper and bottom layers represent the plasma membrane towards the medium and the glass slide, respectively, and the interior region between the two layers stands for intracellular space. It also showed that the intensity of the upper layer was usually stronger than the bottom one, implying the membrane proteins tend to distribute towards the medium environment (Fig. 2Be and Bf). Due to the heterogeneity of primary rat calvarial osteoblast cultures, we evaluated the proportion of cells that showed the difference in subcellular distribution of TRPV4. The percentage of cells with two-layer distribution were 0% and (76.2 ± 8.2) % in day 0 and day 5 groups, respectively (Fig. 2C). Supplementary Fig. S2 provided additional examples of the contrasting distribution changes of TRPV4 during osteoblastic differentiation. Besides, we carried out negative control experiments to establish the specificity of the TRPV4 antibody in supplementary Fig. S3. These results evidently indicated that TRPV4 localization differs in the two differentiation stages of osteoblasts. TRPV4 mainly distributed in intracellular compartment in undifferentiated conditions, but it was predominantly located at the plasma membrane in mature osteoblasts. Overall, our results based on these two methods provided convincing evidences for the plasma membrane translocation of TRPV4 channels during osteoblastic differentiation.

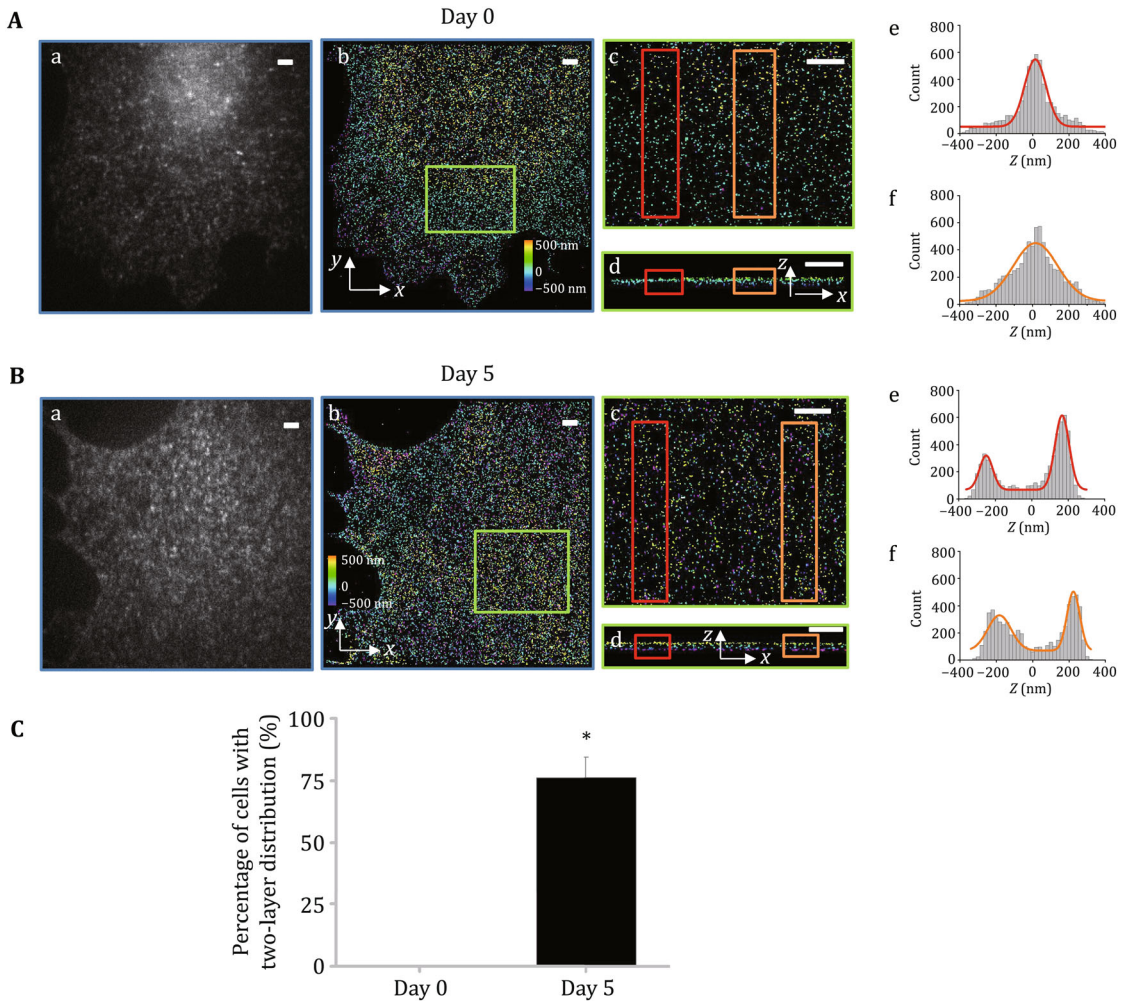

Fig. 2 The plasma membrane translocation of TRPV4 channels in differentiated osteoblasts demonstrated by 3D-STORM imaging. **A** 3D-STORM analysis for TRPV4 distribution in an osteoblast on day 0. **a**, **b** The conventional (**a**) and reconstructed STORM (**b**) image of TRPV4 for an undifferentiated cell. The *z* positions are color coded (color bar). **c** Zoom-in of a selected rectangle region in **b**. **d** STORM image of the selected rectangle region from *z* direction showing a single-layer distribution. **e**, **f** The *z* profiles for two regions along vertical section (*red* and *orange rectangle* in **c**, respectively). Each histogram is fit by Gaussians (*red* and *orange curves*). Scale bar = 2 μm. **B** The 3D-STORM imaging of TRPV4 in an osteoblast cultured in differentiation medium on day 5, indicating a two-layer arrangement of TRPV4. **C** Summary of percentage of cells with two-layer distribution (n = 3), * indicates $P < 0.05$ comparing with day 0 group

Effects of osteoblast differentiation on TRPV4-mediated $[Ca^{2+}]_i$ dynamics

Subsequently, the intracellular Ca^{2+} responses induced by specific TRPV4 agonist GSK1016790A (GSK101) were measured. Results showed that GSK101 dose-dependently triggered $[Ca^{2+}]_i$ increase in osteoblasts both on day 0 (Fig. 3A) and day 5 (Fig. 3B). It is obvious that the Ca^{2+} response amplitude of GSK101-evoked $[Ca^{2+}]_i$ change in differentiated cells (day 5) were stronger than that of undifferentiated cells (day 0) (Fig. 3C), implying a strengthened Ca^{2+} response resulted from differentiation. To investigate the mechanisms underlying the $[Ca^{2+}]_i$ increase, we chose a concentration of 2 nmol/L GSK101 for the following experiments. For cells on day 5, GSK-induced $[Ca^{2+}]_i$ increase was completely abolished in calcium-free buffer (Fig. 3D and E), suggesting that the $[Ca^{2+}]_i$ increase was mostly attributed to extracellular Ca^{2+} entry. On the other hand, the $[Ca^{2+}]_i$ increase was almost eliminated after pretreatment with GSK205 (TRPV4 specific antagonist, 0.5 and 5 μmol/L) and ruthenium red (RR, non-specific TRPV blocker, 0.5 and 5 μmol/L) for 15 min (Fig. 3D and E), revealing that the Ca^{2+} entry elicited by GSK101 relied on the activation of TRPV4. Remarkably, the $[Ca^{2+}]_i$ increase in response to GSK101 caused either an oscillatory or a sustained plateau pattern (supplementary Fig. S4); the former was known to play more important roles in regulating osteoblast gene expression and function (Meng *et al.* 2018; Suzuki *et al.* 2013). As summarized in Fig. 3 and

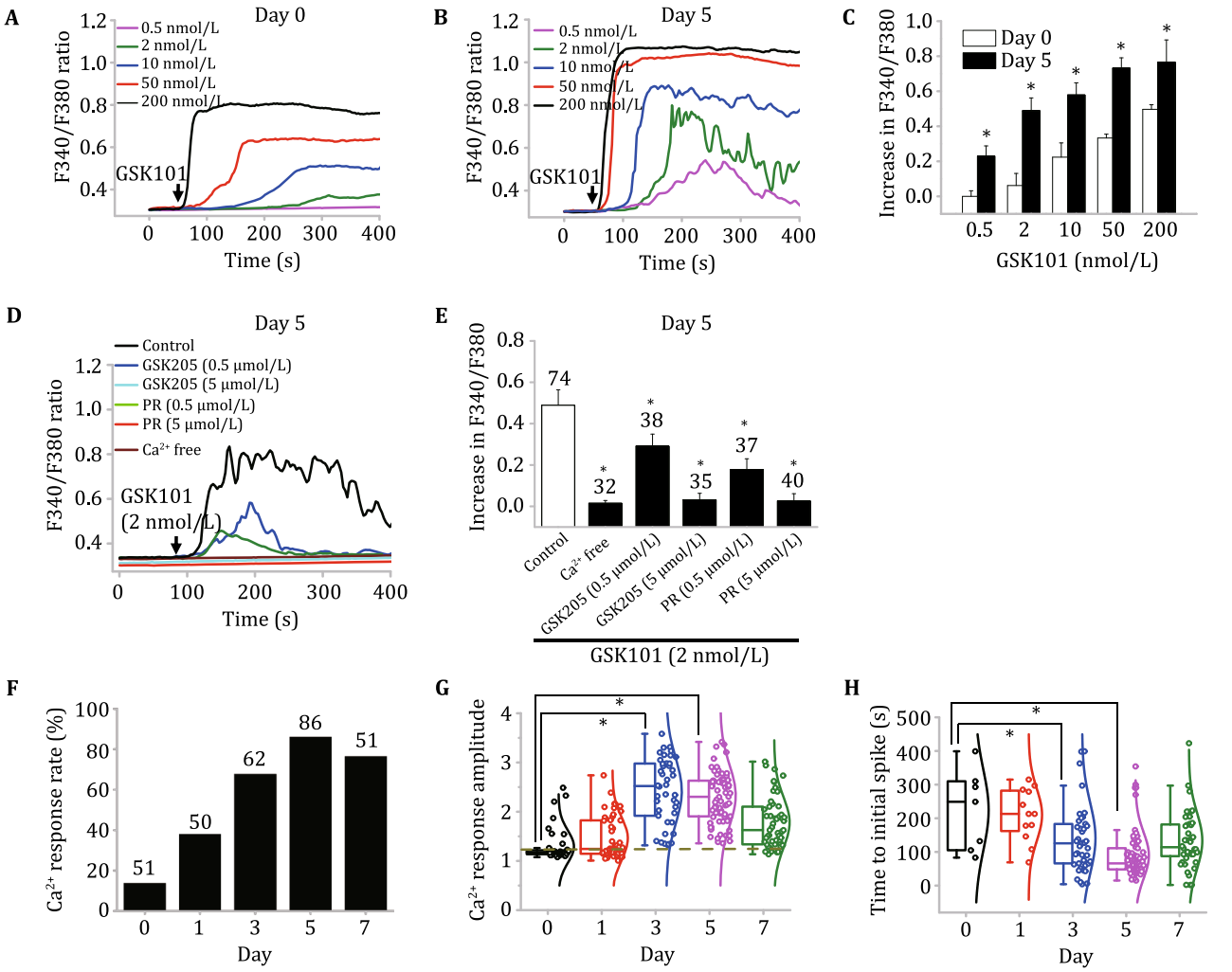

Fig. 3 TRPV4-mediated intracellular Ca^{2+} responses were dependent on osteoblastic differentiation. **A**,**B** Representative $[Ca^{2+}]_i$ traces for stimulating osteoblasts cultured in differentiation medium on day 0 (**A**) and day 5 (**B**) with different doses of GSK101. **C** The statistical values of Ca^{2+} response amplitude (increase in F340/F380 ratio) from experiments are shown in **A** and **B**. * indicates $P < 0.05$ comparing with day 0 group. **D** Typical $[Ca^{2+}]_i$ traces for stimulating osteoblasts cultured in differentiation medium on day 5 with GSK101 (2 nmol/L) in the absence of extracellular Ca^{2+}, or pretreatment with GSK205 (0.5 and 5 μmol/L) and ruthenium red (RR, 0.5 and 5 μmol/L) for 15 min, respectively. **E** Summary of the Ca^{2+} response amplitude after the application of GSK101 from experiments shown in **D**. * indicates $P < 0.05$. **F** Summary of the Ca^{2+} response rate, which means the percentage of cells exhibiting a calcium response (n = 50–80 for each case). **G**,**H** Distribution of Ca^{2+} response amplitude (**G**) and the time to initial spike (**H**) shown in box plot. A cell was defined as responsive if it showed a calcium transient with a peak magnitude not less than 1.25 times of baseline, and the dotted line in **G** showed the value of 1.25. * indicates $P < 0.05$ comparing with day 0 group

supplementary Fig. S4, with prolonged cell differentiation, the Ca^{2+} response rate (Fig. 3F), response amplitude (Fig. 3G) as well as Ca^{2+} oscillation rate (supplementary Fig. S4) induced by GSK101 (2 nmol/L) were significantly increased, while the delay time of Ca^{2+} response was short in day 3 and day 5 groups compared with day 0 group (Fig. 3H). Altogether, these data demonstrated that TRPV4-mediated Ca^{2+} responses were associated with cell differentiation. The membrane translocation of TRPV4 during differentiation hereby provided an explanation for the strengthened Ca^{2+} response in differentiated cells.

Activation of TRPV4 led to rapid phosphorylation of CaMKII in differentiated osteoblasts

In osteoblasts, Ca^{2+} signaling is mainly mediated by the Ca^{2+} binding protein calmodulin (CaM) and CaM-dependent protein kinases (CaMKs), as well as NFAT (Winslow *et al.* 2006; Zayzafoon 2006). Therefore, we tested the activities of CaMKII to further explore the signal downstream of TRPV4-mediated Ca^{2+} influx. Firstly, we examined the expressions of CaMKII and phosphorylated CaMKII (p-CaMKII) simultaneously at different stages of differentiation. The protein levels of

CaMKII and p-CaMKII were almost invariant on day 0–7, with only a slight increase of p-CaMKII in cells on day 5 (Fig. 4A and B). Notably, application with GSK101 (2 nmol/L) for 10 min evoked robust phosphorylation of CaMKII on day 5 in contrast to day 0, whereas it recovered to the base value when treated for 1 h (Fig. 4C and D). In response to GSK101, the phosphorylation of CaMKII was immediately detected after the calcium entry mediated by the activation of TRPV4. Hence, the above results suggest a crucial role of TRPV4 activation for the regulation of CaMKII.

DISCUSSION

The differentiation of osteoblasts is an essential process for bone construction and function (Blair *et al.* 2017; Kassem *et al.* 2008). In this work, it was found that the membrane protein level of TRPV4 in osteoblasts isolated from the calvarias of new born rats was gradually increased, while cytoplasmic protein decreased along with prolonged osteoblastic differentiation (Fig. 1). Then, 3D-STORM results clearly showed a different distribution pattern of TRPV4 in differentiated osteoblasts, which reflected the plasma membrane translocation of TRPV4 (Fig. 2 and supplementary Fig. S2). Further, stimulation with specific TRPV4 agonist GSK101 dose-dependently induced $[Ca^{2+}]_i$ increases due to TRPV4-mediated calcium entry (Fig. 3A–E). The rate and amplitude of GSK101-evoked Ca^{2+} response were dependent on the differentiation of osteoblasts (Fig. 3F–H). These data indicated that the strengthened $[Ca^{2+}]_i$ increases in response to GSK101 should be attributed to the activation of TRPV4 that translocated to the plasma membrane during differentiation. Subsequently, GSK101 induced rapid phosphorylation of CaMKII in differentiated cells (Fig. 4), suggesting that the activation of CaMKII was downstream TRPV4-mediated calcium entry. All these data clearly suggested a pivotal role for TRPV4 membrane translocation during osteogenic differentiation in the modulation of intracellular Ca^{2+}/CaMKII signaling.

Nowadays, mechanosensitive TRP channels have been recognized to be a key sensor and regulator in the development and remodeling of the skeleton (Lieben and Carmeliet 2012); therefore it is important to define their roles in the function of bone cells including osteoblasts. Cellular activity of TRP channels is

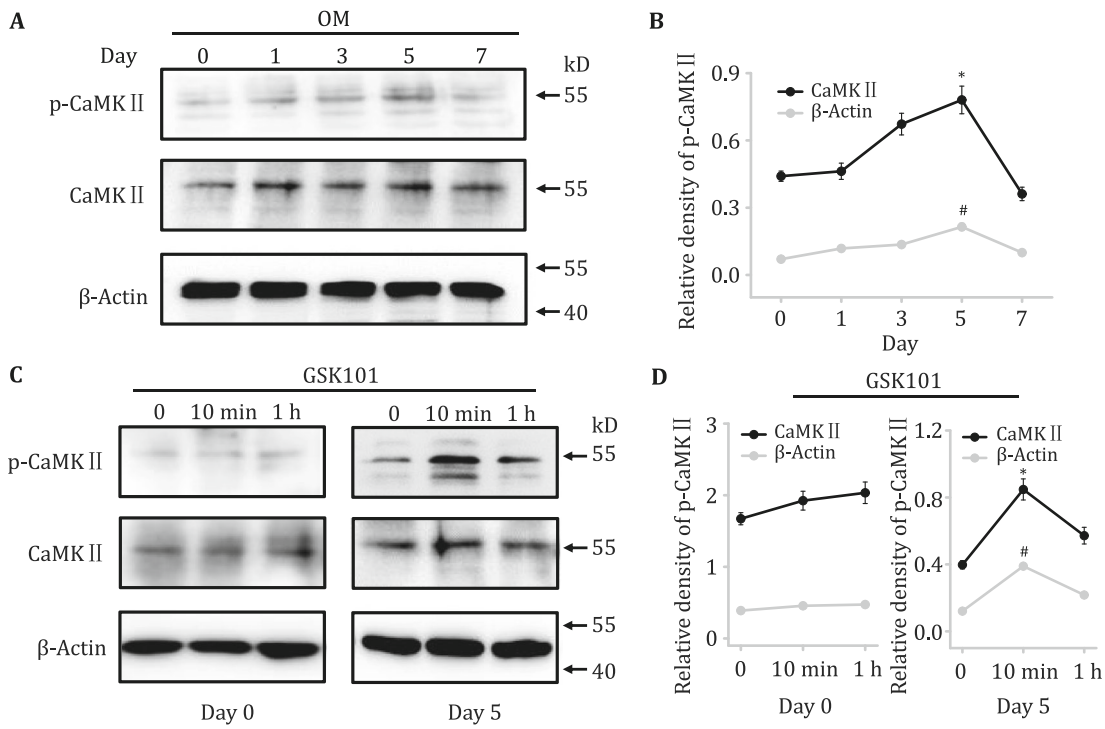

Fig. 4 Effects of TRPV4 activation on CaMKII phosphorylation during osteoblast differentiation. **A** Western blotting bands indicate the expressions of CaMKII and p-CaMKII protein in osteoblasts at different stages of differentiation. **B** Quantitative statistical results of Western blotting in **A** that normalized to the density of CaMKII/β-Actin (n = 3).* and # indicate $P < 0.05$ comparing with day 0 group. **C** Western blotting bands showed the expression of CaMKII and p-CaMKII protein in osteoblasts on day 0 (left) and day 5 (right) applied with GSK101 (2 nmol/L) for different time courses (0 min, 10 min, 1 h). **D** Quantitative statistical results of Western blotting in **C** that normalized to the density of CaMKII/β-Actin (n = 3). * and # indicate $P < 0.05$ comparing with GSK101 0 min group

subjected to a complex modulation encompassing from posttranslational modification to regulation of their abundance at the cell surface (Darby *et al.* 2016). Currently, the transport and mobilization of these channels to the cell membrane are being an area of intense investigation (Ferrandiz-Huertas *et al.* 2014). It has been demonstrated however that TRPV2 channels were stored in intracellular pools such as endoplasmic reticulum in non-stimulated conditions and then get translocated to the plasma membrane and function as a cation channel upon stimulation of the cells by ligands, mechanical stress, or insulin-like growth factor (IGF) (Flockerzi and Nilius 2014). It has also been suggested that TRPM2 translocated to the plasma membrane during microglial activation in response to external stimuli (Echeverry *et al.* 2016). Similarly, we found a translocation process of TRPV4 channels during osteoblastic differentiation based on traditional method—Western blotting (Fig. 1) and powerful 3D super-resolution microscopy (Fig. 2 and supplementary Fig. S2). Due to diffraction limit, traditional fluorescence microscopy can at most provide information at the subcellular level rather than directly monitoring the distribution features of TRPV4 at the single-molecule level. The rise of super-resolution microscopy over the past decade significantly surpass the diffraction limit and achieved a nanoscale lateral/axial resolution (Huang *et al.* 2008), which makes it highly desirable for investigation of spatial organization and distribution of membrane proteins with nanometer precision (AbuZineh *et al.* 2018; Roh *et al.* 2015; Yan *et al.* 2018). Herein, for the first time, we used 3D-STORM super-resolution microscopy to visually and directly explore the localization and distribution pattern of TRPV4 in different stages of osteoblasts, which demonstrated that TRPV4 translocated from intracellular compartments to the plasma membrane during differentiation (Fig. 2 and supplementary Fig. S2).

Furthermore, we found that this membrane translocation of TRPV4 contributed to the modulation of Ca^{2+} response in osteoblasts. Acting as a type of ion channel, the opening of TRPV4 will initially result in the elevation of intracellular Ca^{2+} concentrations ($[Ca^{2+}]_i$), which are crucial for bone homeostasis (Meng *et al.* 2018; Zayzafoon 2006). Activating TRPV4 by its agonist GSK101 triggered significant $[Ca^{2+}]_i$ increases as expected (Fig. 3 and supplementary Fig. S4). Interestingly, the GSK101-elicited Ca^{2+} response in differentiated cells was more rapid and stronger than that of undifferentiated cells (Fig. 3 and supplementary Fig. S4). Given that TRPV4 channels serve as mechanosensor only when they are located on the plasma membrane, the recruitment of TRPV4 to the cell surface may be a crucial step in the physiological functioning of the channel and tightly controlled to ensure the proper regulation of intracellular ion homeostasis and signal transduction. Therefore, the trafficking of TRPV4 to plasma membrane provides a persuasive explanation for the strengthened intracellular Ca^{2+} response triggered by GSK101 in differentiated osteoblasts.

As a critical second messenger, Ca^{2+} regulates a variety of cellular signal transduction. CaM/CaMKII signaling is considered to be one of the most important downstream pathways in osteoblasts (Zayzafoon 2006). Upon binding to Ca^{2+}, CaM undergoes structural changes, allowing it to interact and activate various target proteins including CaMKII. Although CaM/CaMKII signaling has been implicated in TRPV4 activation (Loukin *et al.* 2015; Masuyama *et al.* 2012), relatively little is known about the participation of TRPV4 in the regulation of CaMKII activity. In this work, the activation of TRPV4 by its agonist GSK101 induced rapid phosphorylation of CaMKII in differentiated osteoblasts rather than unstimulated cells (Fig. 4). Since there were more TRPV4 channels localized on the membrane in differentiated cells, our results implicated that the activation of CaMKII was relied on the Ca^{2+} entry mediated by opening TRPV4 at the cell surface. These data together defined a TRPV4 membrane translocation-regulated intracellular Ca^{2+}/CaMKII signaling.

In summary, we demonstrated that osteoblastic differentiation resulted in the translocation of TRPV4 from intracellular space to the plasma membrane. TRPV4 activation by its agonist stimulated Ca^{2+}/CaMKII signaling pathway in osteoblasts, which can be modulated by the membrane abundance of TRPV4 resulted from differentiation. These findings will provide new insights for understanding the mechanisms underlying osteoblastic differentiation and bone remodeling.

MATERIALS AND METHODS

Animals and reagents

New born Sprague–Dawley rats (0–3 day) were obtained from Vital River Laboratory Animal Technology Co., Ltd (Beijing, China, Certification Number: SCXK 2016-0006). Minimum Essential Medium α (α-MEM) and fetal bovine serum (FBS) were from Gibco (USA) and HyClone (USA), respectively. GSK101 and GSK205 were from Millipore (USA). Fura-2/AM was purchased from Biotium (USA). KN-93 was from Selleck (USA). Alizarin red S was from Solarbio (Beijing, China). The rest of reagents, including trypsin, collagenase II, DMSO,

bovine serum albumin (BSA), β-glycerophosphate, ascorbic acid, ruthenium red and EGTA were purchased from Sigma-Aldrich (USA).

Osteoblasts isolation, culture and differentiation

Rat calvarial osteoblasts isolation and culture method was described in our earlier work (Hu *et al.* 2014). Briefly, anesthetized new born rats were sacrificed by decapitation. Then, bone skulls were isolated from the soft tissue and digested with 0.1% collagenase II. Calvarial cells were released by repeated digestion with 0.05% trypsin. The isolated osteoblasts were cultured in α-MEM medium containing 10% FBS at 37 °C with 5% CO_2. For the differentiation assay, osteoblastic induction was performed by culturing primary calvarial cells in osteogenic medium (OM, α-MEM supplementing with 5 mmol/L β-glycerophosphate and 50 μg/mL ascorbic acid) for the indicated time course (Panupinthu *et al.* 2008). The osteogenic medium was replenished every 3 days.

Measurement of intracellular Ca^{2+} concentrations ($[Ca^{2+}]_i$)

Osteoblasts were loaded with 5 μmol/L fura-2/AM in Hanks' balanced salt solution (HBSS) (NaCl 140 mmol/L, KCl 5.4 mmol/L, $CaCl_2$ 2 mmol/L, $MgCl_2$ 1 mmol/L, glucose 10 mmol/L, and HEPES 10 mmol/L, pH 7.4) for 1 h at 37 °C. After washing extensively with HBSS, $[Ca^{2+}]_i$ was measured by calcium imaging system built on an inverted fluorescence microscope (Olympus IX51). The ratiometric Ca^{2+} indicator fura-2 was alternately excited at 340 nm and 380 nm with a Lambda 10-2 Sutter. Fluorescence images (filtered at 515 nm ± 25 nm) were captured by a CCD camera (CoolSNAP fx-M) and analyzed with MetaFluor software. $[Ca^{2+}]_i$ was represented by the ratio of fluorescence intensity at 340 nm/fluorescence intensity at 380 nm (F340/F380). At least three independent experiments were done for each condition. Ca^{2+}-free HBSS solution was made by substituting $MgCl_2$ for $CaCl_2$ at the same concentration with 2 mmol/L EGTA added.

Western blotting for TRPV4 and CaMKII

Osteoblasts were seeded into 10-cm plates (Corning, USA) at 2×10^6 cells per plate and incubated overnight in α-MEM with 10% FBS at 37 °C in prior to various test treatments. Then, the membrane and cytoplasmic protein lysates (for TRPV4) were isolated by a membrane protein isolation kit (Beyotime, China). Briefly, the cells were collected and homogenized to lyse the membrane. After centrifugation at 700 *g*, the supernatant was collected to remove the nucleus and insufficient lytic cells. The supernatant was then centrifuged at 14,000 *g* to precipitate cell membranes and the consequent supernatant containing cytoplasmic protein was collected. Finally, membrane protein extraction reagent was used for the extraction of membrane proteins. Total protein lysates (for CaMKII) were isolated by RIPA (Beyotime, China). The concentration of protein was determined using a BCA assay kit (Beyotime, China). After that, aliquots (20 μg/lane) were separated by 10% SDS-PAGE and transferred to a nitrocellulose membrane, then blocked non-specific binding sites with 5% BSA at room temperature for 1 h, immunoblotted with anti-TRPV4 (1:200, ACC-034, Alomone labs, Israel), anti-CaMKII and anti-phosphorylated CaMKII (1:1000, 11945S and 12716S, Cell Signaling Technology, USA), as well as mouse anti-β-actin (1:20,000, 60,008-1-lg, Proteintech, USA) overnight at 4 °C, followed by incubation with anti-rabbit/mouse horseradish peroxidase-conjugated secondary antibody (1:1000, A0208/A0216, Beyotime, China). Finally, the ECL detection reagent (Proteintech, USA) was used for visualization in Tanon 5200 MultiImage System.

Immunofluorescence of TRPV4 by 3D super-resolution microscopy

Our super-resolution microscopy is 3D stochastic optical reconstruction microscopy (3D-STORM) with 25 nm lateral resolution and 50 nm axial resolution. Osteoblasts cultured in osteogenic medium for the indicated days were seeded on 12-mm glass cover slips in a 24-well plate (Corning, USA) at 2×10^4 cells per well, incubated for 12 h before immunostaining. After being fixed with 4% paraformaldehyde in phosphate buffered saline (PBS) for 20 min, the samples were permeabilized and blocked in blocking buffer (3% BSA, 0.5% Triton X-100 in PBS) for 20 min. the cells were then incubated with a polyclonal antibody against a peptide corresponding to residues 853–871 of rat TRPV4 (1:100, ACC-034, Alomone labs, Israel) for 1 h at room temperature. After washing for three times, the cells were incubated with the secondary antibody Alexa Fluor® 647 goat anti-rabbit IgG (H + L) (1:400, A21245, ThermoFisher, USA) for 1 h. For 3D-STORM imaging, the samples were mounted on glass slides using an imaging buffer containing 5% glucose, 100 mmol/L cysteamine, 0.8 mg/mL glucose oxidase, and 40 μg/mL catalase in Tris–HCl (pH 7.5) after extensive washing. Fluorescence images were collected via a homebuilt STORM setup based on an inverted optical microscope (Nikon Eclipse Ti-E) equipped with

an EMCCD (Andor iXon Ultra 897) (Pan *et al.* 2018). The image stacks with ~50,000 frames per image were used to determine the location of each TRPV4 protein using the localization algorithm described previously (Huang *et al.* 2008), in which the centroid positions and ellipticities of the single-molecule images obtained in each frame were respectively used to deduce the lateral and axial positions of each molecule.

Quantitative real-time PCR (qRT-PCR)

Total RNA was extracted from osteoblasts using the RNAprep pure Cell/Bacteria Kit (Tiangen Biotech, China) following the manufacturer's instructions. One microgram of isolated RNA was reverse transcribed to cDNA using the PrimeScript™RT Master Mix (Takara, Japan) according to the manufacturer's protocols. Then, qRT-PCR was conducted with SYBR® Premix Ex Taq™ II (Tli RNaseH Plus) (Takara, Japan). Fold gene expression was determined by first normalization to GAPDH, and then normalization to day 0 group. Sequences of gene-specific primers (Table 1) were designed using the Primer 5 (Premier Biosoft, USA) and evaluated with Oligo 7 (Molecular Biology Insights, USA).

Statistical analysis

All data are presented as mean ± standard deviation (SD) from at least three independent experiments. The statistical comparison between two groups was carried out using Student's *t* test (Origin 8.1) and the analysis for multiple groups using Dunnett's test (SPSS 18.0, one-way ANOVA). $P < 0.05$ was considered to be statistically significant.

Table 1 Primers used to detect genes in osteoblasts by qRT-PCR

Gene	PubMed acc. no.	Sequence	
TRPV4	NM_023970.1	F:	GAGGAGGAAGGTCGTAGAGAAG
		R:	TCAGCAAGTAGGAGAGCAGTC
PACSIN3	NM_001009966.2	F:	TGGCACGCCTTCTTCACT
		R:	GACCATGCAACTTCTCCCTC
ALPL	NM_013059.1	F:	GTCTGGAACCGCACTGAAC
		R:	AAGCCTTTGGGATTCTTTGT
BSP	NM_012587.2	F:	ACGGGTTTCAGCAGACGA
		R:	CATAGGTTTCATACGCAGTGTT
RUNX2	NM_001278483.1	F:	ACGTACCCAGGCGTATTTC
		R:	GTGAAGGTGGCTGGATAGTG
OSX	NM_181374.2	F:	CAATGACTACCCACCCTTTCC
		R:	ATGGATGCCCGCCTTGTA
GAPDH	NM_017008.4	F:	GTGCTGAGTATGTCGTGGAGTC
		R:	TTGCTGACAATCTTGAGGGA

Acknowledgements This work was supported by the National Natural Science Foundation of China (11874231, 11574165 and 31801134), Tianjin Natural Science Foundation (18JCQNJC02000), the PCSIRT (IRT_13R29), and the 111 Project (B07013).

Compliance with Ethical Standards

Conflict of interest Fen Hu, Yali Zhao, Zhenhai Hui, Fulin Xing, Jianyu Yang, Imshik Lee, Xinzheng Zhang, Leiting Pan and Jingjun Xu declare that they have no conflict of interest.

Human and animal rights and informed consent All institutional and national guidelines for the care and use of laboratory animals were followed.

References

Abed E, Labelle D, Martineau C, Loghin A, Moreau R (2009) Expression of transient receptor potential (TRP) channels in human and murine osteoblast-like cells. Mol Membr Biol 26:146–158

AbuZineh K, Joudeh LI, Al Alwan B, Hamdan SM, Merzaban JS, Habuchi S (2018) Microfluidics-based super-resolution microscopy enables nanoscopic characterization of blood stem cell rolling. Sci Adv 4:5304

Blair HC, Larrouture QC, Li Y, Lin H, Beer-Stoltz D, Liu L, Tuan RS, Robinson LJ, Schlesinger PH, Nelson DJ (2017) Osteoblast differentiation and bone matrix formation *in vivo* and *in vitro*. Tissue Eng Part B 23:268–280

Christensen AP, Corey DP (2007) TRP channels in mechanosensation: direct or indirect activation? Nat Rev Neurosci 8:510–521

Crockett JC, Rogers MJ, Coxon FP, Hocking LJ, Helfrich MH (2011) Bone remodelling at a glance. J Cell Sci 124:991–998

Cuajungco MP, Grimm C, Oshima K, D'hoedt D, Nilius B, Mensenkamp AR, Bindels RJ, Plomann M, Heller S (2006) PACSINs bind to the TRPV4 cation channel. PACSIN 3 modulates the subcellular localization of TRPV4. J Biol Chem 281:18753–18762

Darby WG, Grace MS, Baratchi S, McIntyre P (2016) Modulation of TRPV4 by diverse mechanisms. Int J Biochem Cell Biol 78:217–228

Echeverry S, Rodriguez MJ, Torres YP (2016) Transient receptor potential channels in microglia: roles in physiology and disease. Neurotox Res 30:467–478

Ehrlich PJ, Lanyon LE (2002) Mechanical strain and bone cell function: a review. Osteoporos Int 13:688–700

Ferrandiz-Huertas C, Mathivanan S, Wolf CJ, Devesa I, Ferrer-Montiel A (2014) Trafficking of ThermoTRP Channels. Membranes (Basel) 4:525–564

Flockerzi V, Nilius B (2014) TRPs: truly remarkable proteins. Handb Exp Pharmacol 222:1–12

Garcia-Elias A, Mrkonjić S, Jung C, Pardo-Pastor C, Vicente R, Valverde MA (2014) The TRPV4 channel. Handb Exp Pharmacol 222:293–319

Guilak F, Leddy HA, Liedtke W (2010) Transient receptor potential vanilloid 4: the sixth sense of the musculoskeletal system? Ann N Y Acad Sci 1192:404–409

Gundberg CM (2000) Biochemical markers of bone formation. Clin Lab Med 20:489–501

Hu F, Pan L, Zhang K, Xing F, Wang X, Lee I, Zhang X, Xu J (2014) Elevation of extracellular Ca^{2+} induces store-operated calcium entry via calcium-sensing receptors: a pathway contributes to the proliferation of osteoblasts. PLoS One 9:e107217

Huang B, Wang W, Bates M, Zhuang X (2008) Three-dimensional super-resolution imaging by stochastic optical reconstruction microscopy. Science 319:810–813

Kang SS, Shin SH, Auh CK, Chun J (2012) Human skeletal dysplasia caused by a constitutive activated transient receptor potential vanilloid 4 (TRPV4) cation channel mutation. Exp Mol Med 44:707–722

Kassem M, Abdallah BM, Saeed H (2008) Osteoblastic cells: differentiation and trans-differentiation. Arch Biochem Biophys 473:183–187

Katagiri T, Takahashi N (2002) Regulatory mechanisms of osteoblast and osteoclast differentiation. Oral Dis 8:147–159

Leddy HA, McNulty AL, Guilak F, Liedtke W (2014) Unraveling the mechanism by which TRPV4 mutations cause skeletal dysplasias. Rare Dis 2:e962971

Lieben L, Carmeliet G (2012) The involvement of TRP channels in bone homeostasis. Front Endocrinol (Lausanne) 20:99

Long F (2011) Building strong bones: molecular regulation of the osteoblast lineage. Nat Rev Mol Cell Biol 13:27–38

Loukin SH, Teng J, Kung C (2015) A channelopathy mechanism revealed by direct calmodulin activation of TrpV4. Proc Natl Acad Sci USA 112:9400–9405

Marie PJ (2008) Transcription factors controlling osteoblastogenesis. Arch Biochem Biophys 473:98–105

Masuyama R, Vriens J, Voets T, Karashima Y, Owsianik G, Vennekens R, Lieben L, Torrekens S, Moermans K, Vanden Bosch A, Bouillon R, Nilius B, Carmeliet G (2008) TRPV4-mediated calcium influx regulates terminal differentiation of osteoclasts. Cell Metab 8:257–265

Masuyama R, Mizuno A, Komori H, Kajiya H, Uekawa A, Kitaura H, Okabe K, Ohyama K, Komori T (2012) Calcium/calmodulin-signaling supports TRPV4 activation in osteoclasts and regulates bone mass. J Bone Miner Res 27:1708–1721

Maycas M, Esbrit P, Gortázar AR (2017) Molecular mechanisms in bone mechanotransduction. Histol Histopathol 32:751–760

Meng G, Li C, Sun H, Lee I (2018) Multiple calcium patterns of rat osteoblasts under fluidic shear stress. J Orthop Res 36:2039–2051

Nilius B, Vriens J, Prenen J, Droogmans G, Voets T (2004) TRPV4 calcium entry channel: a paradigm for gating diversity. Am J Physiol Cell Physiol 286:C195–C205

O'Conor CJ, Griffin TM, Liedtke W, Guilak F (2013) Increased susceptibility of Trpv4-deficient mice to obesity and obesity-induced osteoarthritis with very high-fat diet. Ann Rheum Dis 72:300–304

O'Conor CJ, Leddy HA, Benefield HC, Liedtke WB, Guilak F (2014) TRPV4-mediated mechanotransduction regulates the metabolic response of chondrocytes to dynamic loading. Proc Natl Acad Sci USA 111:1316–1321

Pan L, Yan R, Li W, Xu K (2018) Super-resolution microscopy reveals the native ultrastructure of the erythrocyte cytoskeleton. Cell Rep 22:1151–1158

Panupinthu N, Rogers JT, Zhao L, Solano-Flores LP, Possmayer F, Sims SM, Dixon SJ (2008) $P2X_7$ receptors on osteoblasts couple to production of lysophosphatidic acid: a signaling axis promoting osteogenesis. J Cell Biol 181:859–871

Raggatt LJ, Partridge NC (2010) Cellular and molecular mechanisms of bone remodeling. J Biol Chem 285:25103–25108

Roh KH, Lillemeier BF, Wang F, Davis MM (2015) The coreceptor CD4 is expressed in distinct nanoclusters and does not colocalize with T-cell receptor and active protein tyrosine kinase p56lck. Proc Natl Acad Sci USA 112:E1604–E1613

Suzuki T, Notomi T, Miyajima D, Mizoguchi F, Hayata T, Nakamoto T, Hanyu R, Kamolratanakul P, Mizuno A, Suzuki M, Ezura Y, Izumi Y, Noda M (2013) Osteoblastic differentiation enhances expression of TRPV4 that is required for calcium oscillation induced by mechanical force. Bone 54:172–178

van der Eerden BC, Oei L, Roschger P, Fratzl-Zelman N, Hoenderop JG, van Schoor NM, Pettersson-Kymmer U, Schreuders-Koedam M, Uitterlinden AG, Hofman A, Suzuki M, Klaushofer K, Ohlsson C, Lips PJ, Rivadeneira F, Bindels RJ, van Leeuwen JP (2013) TRPV4 deficiency causes sexual dimorphism in bone metabolism and osteoporotic fracture risk. Bone 57:443–454

White JP, Cibelli M, Urban L, Nilius B, McGeown JG, Nagy I (2016) TRPV4: molecular conductor of a diverse orchestra. Physiol Rev 96:911–973

Winslow MM, Pan M, Starbuck M, Gallo EM, Deng L, Karsenty G, Crabtree GR (2006) Calcineurin/NFAT signaling in osteoblasts regulates bone mass. Dev Cell 10:771–782

Xu H, Fu Y, Tian W, Cohen DM (2006) Glycosylation of the osmoresponsive transient receptor potential channel TRPV4 on Asn-651 influences membrane trafficking. Am J Physiol Renal Physiol 290:F1103–F1109

Yan Q, Lu Y, Zhou L, Chen J, Xu H, Cai M, Shi Y, Jiang J, Xiong W, Gao J, Wang H (2018) Mechanistic insights into GLUT1 activation and clustering revealed by super-resolution imaging. Proc Natl Acad Sci USA 115:7033–7038

Zaidi M (2007) Skeletal remodeling in health and disease. Nat Med 13:791–801

Zayzafoon M (2006) Calcium/calmodulin signaling controls osteoblast growth and differentiation. J Cell Biochem 97:56–70